PHYSICAL REVIEW B **77**, 161304(R) (2008)

Light-induced solid-to-solid phase transformation in Si nanolayers of Si-SiO_2 multiple quantum wells

T. Mchedlidze,* T. Arguirov, S. Kouteva-Arguirova, and M. Kittler
IHP Microelectronics, Im Technologiepark 25, D-15236 Frankfurt (Oder), Germany
and IHP/BTU Joint Laboratory, Konrad-Wachsmann-Allee 1, D-03046 Cottbus, Germany

R. Rölver, B. Berghoff, D. L. Bätzner, and B. Spangenberg
Institute of Semiconductor Electronics, RWTH Aachen University, D-52074 Aachen, Germany
(Received 4 March 2008; published 11 April 2008)

Amorphous Si was completely transformed to a nanocrystalline phase in nanometer thick layers of Si-SiO_2 multiple quantum wells deposited on quartz substrates employing an illumination with a continuous-wave laser. The process was controlled by micro-Raman spectroscopy. Preferential heating of amorphous Si due to selective light absorption in the employed range of laser radiation wavelengths and solid-to-solid phase transformation can explain the obtained results.

DOI: 10.1103/PhysRevB.77.161304 PACS number(s): 68.65.Fg, 64.70.kg, 78.30.Am, 78.67.De

Multiple quantum well (MQW) structures containing nanometer-thick alternating crystalline Si and isolating layers, individual Si-nanowires and those assembled in networks, and Si-quantum dots are examples of nanostructures to be used in microelectronics, photonics, photovoltaics, bioelectronics, etc., in the future due to expected quasidirect and controllable band-gap and advanced carrier-transport properties.[1–5] Bearing in mind the compatibility of the Si nanostructures with modern semiconductor technology, perspectives for their prompt integration in the actual devices are very good. The hitherto unresolved problem was poor crystalline quality for extended one-dimensional (1D) and two-dimensional (2D) Si nanostructures.[6]

Despite the broad interest and large number of investigations in the area of phase transitions in Si (see Refs. 7–11, and references therein), the topic is still far from being clear. The formation and growth of crystalline inclusions in an amorphous matrix, so-called solid-to-solid phase transformation (SSPT), is an interesting fundamental problem.[12] Transition of a-Si to crystalline in free standing Si films at temperatures below the melting point (see Ref. 13, and references therein) represents an example of SSPT in a monatomic system. The growth of Si-nanocrystals (Si-nc) in an amorphous Si (a-Si) matrix was also considered recently in Refs. 14 and 15. Below we will present results describing light-induced SSPT of nanometer-thick a-Si layers in Si-SiO_2 MQWs deposited on quartz substrate. Differently from the broadly investigated laser annealing of a-Si (see Refs. 16–18, and references therein), the melting of the material does not occur when the proper parameters of illumination are used and complete a-Si$\rightarrow$Si-nc SSPT could be achieved.

The preparation of a Si-SiO_2 MQW implies crystallization of a-Si in stacks of Si and SiO_2 layers deposited on a substrate.[6] Several methods, i.e., furnace annealing, rapid thermal annealing (RTA), laser annealing, and their combinations have been applied for the crystallization of the a-Si layers previously.[6,19–22] An interaction of several materials in a MQW having different thermal properties, i.e., Si-nc, a-Si, SiO_2, and a substrate, during the heat treatments is an obvious source for problems with crystallization. Besides that, in a Si-SiO_2 MQW at high temperatures atoms from Si layers may dissolve in silicon dioxide forming a SiO_x ($x<2$) phase and causing the appearance of compressive stress in the system. Changes in the volumes of the materials in the MQW, i.e., variations in thickness of layers and/or in the number of periods, also affect the crystallization process. Hitherto the complete crystallization of Si layers in the MQW on a substrate for a wide range of Si layer thicknesses was not achieved and in most cases only $<60\%$ of a-Si could be crystallized.[6,23–26]

From our recent investigations of Si-SiO_2 MQW structures [24,25] it became possible to determine factors governing the crystallization process in Si-SiO_2 MQW structures. These investigations showed that application of traditional crystallization methods based on melting-solidification cycles face enormous problems in the case of the multimaterial systems. It was suggested that only proper design of MQW structure and tuning of the thermal treatment parameters to a specific MQW may substantially improve the level of crystallinity.[24] Recently promising results were reported for the laser annealing of free-standing MQW films (see Ref. 26, and references therein). The results related to laser treatments of a Si-SiO_2 MQW[25,26] indicated the existence of a mechanism allowing complete a-Si$\rightarrow$Si-nc transformation.

Remote plasma-enhanced chemical vapor deposition (RPECVD) was employed for fabrication of Si-SiO_2 MQWs on quartz substrate.[19] The thickness of a-Si layers was varied from 3 to 10 nm for various MQWs and the thickness of the SiO_2 layers was kept constant at 3 nm. The number of Si-SiO_2 periods was also varied. Below, to specify the MQW structure we will use the following notation $n(d\ \mathrm{Si}+b\ \mathrm{SiO_2})$, where n is the number of periods, d is the deposited Si layer thickness in nm and b is that for SiO_2 layers. As-deposited MQWs were subjected to laser treatments, i.e., the MQW surface was illuminated with a laser radiation in air. The laser was focused to a spot with $\sim 1\ \mu m^2$ area using the system employed for the Raman measurements. Various wavelengths of an Ar^+ cw laser, i.e., 514, 488, 457, and 532 nm radiation from a frequency doubled Nd:YVO_4 cw laser were employed for the treatments. Controlled move-

ment of the sample allowed laser treatment of extended areas, i.e., up to 300×300 μm^2.

Traditional methods for structural investigation of materials include x-ray diffraction, transmission electron microscopy (TEM), and Raman spectroscopy (RS). Due to insufficient volumes of the laser-treated material, employment of x-ray diffraction was impossible in our case. RS is widely acknowledged as an experimental method allowing sensitive and versatile investigation of Si-nc structures (see Refs. 6 and 21–30, and references therein). Differently from TEM, RS probes a much larger volume of samples, thus allowing detection of small residual a-Si inclusions in the crystallized material. Moreover, sample preparation procedures which are necessary for TEM analyses can induce amorphization of Si-nc, thus burdening interpretation of the results. Besides detection of a-Si, Si-nc, and high pressure phases of Si (Ref. 7), RS allows determination of Si crystallite dimensions from the full width at half maximum (FWHM) of the Si-nc Raman peak (see Refs. 24, 27, and 28, and references therein). Similar information is contained also in spectral position (wave number) of the Si-nc Raman peak maximum, ν_{MAX}. However, ν_{MAX} is also affected by the internal stress in a sample.[28,29] Thus comparing the FWHM and ν_{MAX} results, information about a resulting stress in the sample could be obtained. The integrated intensity of Si-nc, I_{Si-nc}, and that of a-Si Raman signals, I_{a-Si} is proportional to relevant fractions of the materials. Thus the crystalline fraction of the Si-nc material could be estimated using the $F_{CR}=(I_{Si-nc})/(I_{Si-nc}+I_{a-Si})$ expression.[17,30]

The mean size of the Si-nc, the crystalline fraction, and the residual stress in MQWs were estimated from results of RS investigations of as-deposited and laser treated MQW samples. Raman spectra with a spectral resolution 0.05 cm^{-1} were recorded employing a micro-Raman spectrometer (Dilor XY) equipped with a frequency doubled Nd:YVO_4 cw laser. We used low power density of the probe beam ($<1.4\times10^5$ W/cm^2) to minimize local heating of the samples during the measurements.

Raman spectra detected from 20(3Si+3SiO_2) MQW after various laser treatments are presented in Fig. 1. The treatments were performed at neighboring locations of the MQW using laser radiation at $\lambda_{LAS}=532$ nm. The values of the radiation power during the treatments,[31] P_{LAS}, are indicated in the figure. The formation of Si-nc upon laser treatment, evidenced by the appearance and growth of a Si-nc related peak at ~520 cm^{-1}, was accompanied by a decrease in the intensity of signal related to a-Si. Namely, a broad feature with a maximum at ~480 cm^{-1} related to a-Si (see curve corresponding to <3 mW) gradually disappeared upon increasing the laser power. The intensity of the Si-nc related signal reached the maximum at $P_{LAS}=3.8$ mW and decreased for larger P_{LAS} values, and finally approached the detection limit at $P_{LAS}>10$ mW. Similar results were obtained for 12(5Si+3SiO_2) and 6(10Si+3SiO_2) MQW structures. However, P_{LAS} values necessary to obtain the maximal I_{Si-nc} showed strong dependence on the Si layer thickness in MQW.

The laser radiation wavelength λ_{LAS} also strongly affected the crystallization process. The dependencies of I_{Si-nc} and F_{CR} from P_{LAS} at various λ_{LAS} in the 6(10Si+3SiO_2) MQW are presented in Fig. 2. It is seen that the F_{CR} value increased

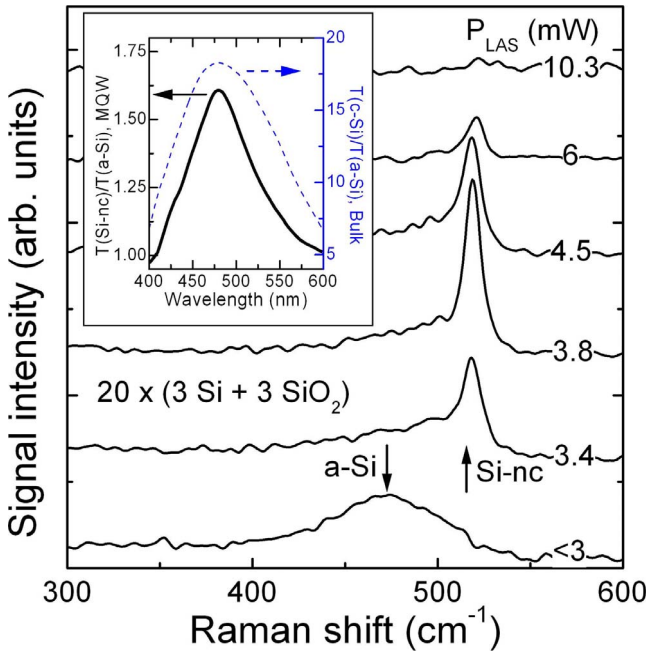

FIG. 1. (Color online) Evolution of Raman spectra for a 20(3Si+3SiO_2) MQW with variation of P_{LAS} at 532 nm. Attribution of Raman features and employed P_{LAS} are indicated in the figure. The spectra are shifted on the vertical axis for clarity of presentation. Inset shows light transmittance ratio T(Si-nc)/T(a-Si) in the range 400–600 nm for the MQW subjected to laser treatments at $P_{LAS}=3.8$ mW. Dotted line shows T(c-Si)/T(a-Si) from Ref. 32.

with P_{LAS}, and $F_{CR\cong1}$ was achieved for every employed λ_{LAS}. However, the maximal values of I_{Si-nc} differ for various λ_{LAS} and were reached at various P_{LAS}. An optimal P_{LAS} can be found for each λ_{LAS} where the Si layers are nearly crystalline ($F_{CR\cong1}$) and I_{Si-nc} is on maximum for given λ_{LAS}. The optimal P_{LAS} decreased for smaller λ_{LAS}. Moreover, from Fig. 2 we conclude that for obtaining maximal volume of Si-nc, λ_{LAS} also should have an optimal value. Namely, the maximal value of I_{Si-nc} was obtained at $P_{LAS}=26$ mW and $\lambda_{LAS}=514$ nm for 6(10Si+3SiO_2) MQW.

The observed dependence on λ_{LAS} may be attributed to a difference in light absorption between a-Si and Si-nc layers in MQW. To estimate the difference we compared light intensity transmitted through small areas (~10 μm^2) of a laser-treated or/and as-deposited MQW sample. For these measurements an incandescent lamp served as a light source and the monochromator and the detector of the Raman installation were employed as a registration system. The ratio of the transmittance of Si-nc to a-Si layers were calculated from these measurements for the wavelength range 400–600 nm and are presented in the inset of Fig. 1 for 20(3Si+3SiO_2) MQW after treatment with 3.8 mW at $\lambda_{LAS}=532$ nm. For comparison, the ratio of the transmittance in c-Si and a-Si is also presented in the inset, which was estimated from the results published in Refs. 26 and 32. As seen from the figure, both ratios exhibit maxima at ~490 nm.

The dependencies of Si-nc sizes and of the resulting stress in the 6(10Si+3SiO_2) MQW on P_{LAS} at $\lambda_{LAS}=532$ nm, estimated from the obtained Raman spectra using previously

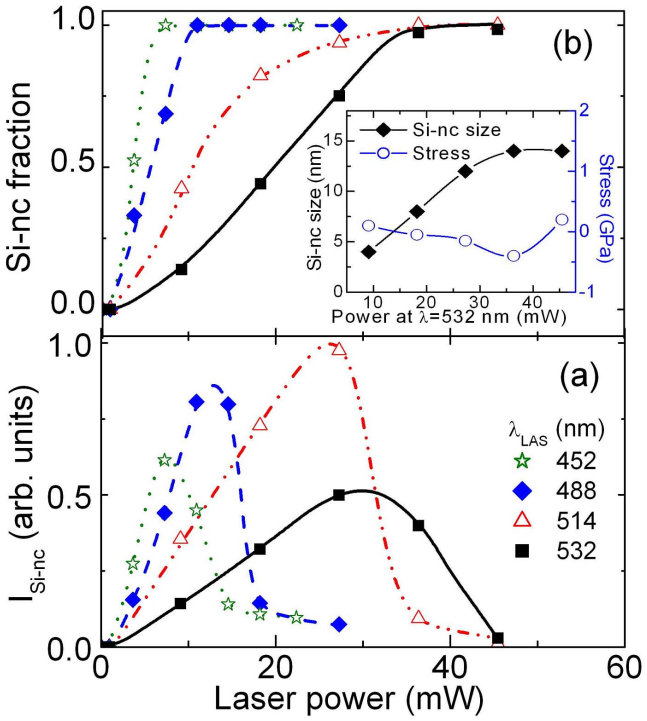

FIG. 2. (Color online) Dependence of the intensity of the Si-nc related peak in the Raman spectra (a) and the crystalline fraction value (b) on the P_{LAS} for the various λ_{LAS} for a 6(10Si+3SiO$_2$) MQW. Attribution of symbols is indicated in the figure. Curves are shown to guide the eye. Inset presents values for Si-nc size and stress in a MQW.

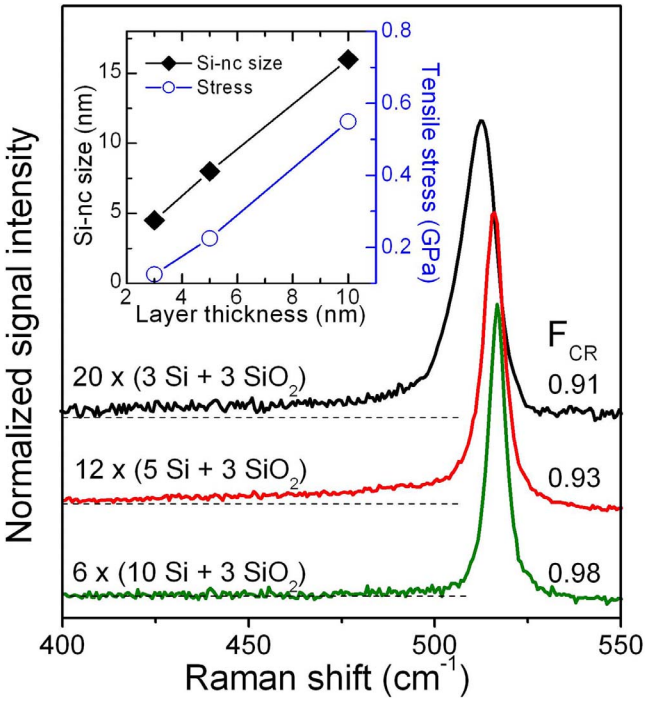

FIG. 3. (Color online) Raman spectra detected from various MQWs crystallized in nearly optimal conditions of laser radiation. Values for crystalline fraction are indicated in the figure. Inset presents sizes of Si-nc crystallites and stress in the MQWs estimated from Si-nc peak characteristics.

published dependencies,[27–29] are presented in the inset of Fig. 2. The sizes of Si-nc increased up to P_{LAS}=40 mW, despite the decrease in I_{Si-nc} after P_{LAS}=30 mW. Moreover, for $P_{LAS}>30$ mW the Si-nc average size exceeds the deposited a-Si layer thickness. We suppose that large Si crystallites with dimensions exceeding the layer thickness were formed planarily in the layers. The emergence of tensile stress in the system should be related to a volume reduction during the a-Si→Si-nc transformation process.[11] At powers $P_{LAS}>40$ mW on λ_{LAS}=532 nm we observed a sharp decrease in the overall Si-related Raman signal, an increase of the residual a-Si signal, and emergence of the compressive stress. The spectra resembled those detected after conventional laser annealing of a-Si[16–18] or those detected in thermally treated MQWs.[6,20–22,24]

The time of the laser treatment in the range t_{LAS} =1–300 s played only a minor role for the transformation. For given λ_{LAS} and constant P_{LAS}, variation of t_{LAS} did not cause changes in I_{Si-nc} nor in F_{CR} values (due to technical problems it was not possible to investigate the $t_{LAS}<1$ s range). Only a blueshift in the Si-nc Raman peak position for constant FWHM value was observed with the increase in the laser-treatment time, which could be attributed to stress relaxation of the Si-nc by the mechanism proposed in Refs. 25 and 26.

Further investigations will be necessary to propose a quantitative mechanism for a-Si→Si-nc transformation in a Si-SiO$_2$ MQW. The coincidence of the optimal value for the λ_{LAS} with that for the maximal difference in light absorption between a-Si and Si-nc (see inset in Fig. 1) hint on a qualitative picture. Namely, selective absorption of light leads to heating and expansion of a-Si, causing increase in the pressure and to a-Si→Si-nc transformation at certain P_{LAS}. After the transformation, the MQW becomes more transparent, providing a negative feedback for the light absorption, hence further heating is reduced and melting of Si does not occur. Low power densities of illumination[31] necessary for complete a-Si→Si-nc transformation suggest a SSPT mechanism for the process. Since the laser heating reaches steady state very rapidly,[33] the a-Si→Si-nc transformation is finished within several milliseconds and overall heating of the system is small. This supposition agrees with the absence of the process dependence on the treatment time for $t_{LAS}>1$ s. From the other side, the transformation could occur in a part of the volume subjected to the illumination and probably the optimal P_{LAS} corresponds to the transformation of the whole illuminated a-Si material. Further increase in P_{LAS} may cause significant heating of Si-nc itself, melting of Si, dissolution of Si atoms in SiO$_2$, and formation of SiO$_x$.

Various MQWs were crystallized in our experiments under nearly optimal conditions. Raman spectra after the laser treatments are presented in Fig. 3. It should be noted that number of periods, total thickness of Si material, and thickness of SiO$_2$ layers in a MQW does not affect the SSPT process. Namely in our preliminary experiments 4(5Si +3SiO$_2$), and monolayers 1(10Si+5SiO$_2$), 1(4Si+5SiO$_2$), and 1(3Si+5SiO$_2$) were also crystallized with $F_{CR}>0.9$.

The inset in Fig. 3 shows Si-nc sizes and stresses in MQW. Again, the Si-nc size exceeding the thickness of the deposited layers suggests the planar growth mechanism of Si-nc in the layers. As it can be expected, the tensile stress increased with the thickness of the transformed layer.

Summarizing the obtained results, a-Si→Si-nc conversion occurred due to the self-regulating process of light-induced solid-to-solid phase transformation in Si-SiO_2 MQW deposited on a quartz substrate. Power density and wavelength of irradiation were critical parameters of the process, while treatment time played only a minor role for the treatment periods exceeding 1 s. Proper selection of the irradiation parameters allowed complete conversion of a-Si to Si-nc independently from the parameters of the MQW.

This work was partly funded by the European Commission under the frame of SINANO (IST-506844) and by the BMBF, Germany, under Contract No. 03SF0308.

*Corresponding author. IHP/BTU JointLab, BTU, Konrad-Wachsmann-Allee 1, Cottbus, Germany. FAX: 49355-694961. teimuraz.mtchedlidze@tu-cottbus.de

[1] L. T. Canham, Appl. Phys. Lett. **57**, 1046 (1990).
[2] L. Pavesi, J. Phys.: Condens. Matter **15**, R1169 (2003).
[3] D. J. Sirbuly, M. Law, H. Yan, and P. Yang, J. Phys. Chem. B **109**, 15190 (2005).
[4] A. P. Alivisatos, Science **271**, 933 (1996).
[5] Y. Wu, C. Yang, W. Lu, and C. M. Lieber, Nature (London) **430**, 61 (2004).
[6] T. Zheng and Z. Li, Superlattices Microstruct. **37**, 227 (2005).
[7] V. Domnich and Y. Gogotsi, Rev. Adv. Mater. Sci. **3**, 1 (2002).
[8] M. Kaczmarski, O. N. Bedoya-Martínez, and E. R. Hernandez, Phys. Rev. Lett. **94**, 095701 (2005).
[9] C. C. Yang, J. C. Li, and Q. Jiang, Solid State Commun. **129**, 437 (2004).
[10] M. Durandurdu and D. A. Drabold, Phys. Rev. B **64**, 014101 (2001).
[11] M. Durandurdu and D. A. Drabold, Phys. Rev. B **67**, 212101 (2003).
[12] L. D. Landau and E. M. Lifshitz, *Statistical Physics* (Butterworth-Heinemann, Oxford, 1980).
[13] O. Schoenfeld, T. Hempel, and J Bläsing, Phys. Status Solidi A **143**, 323 (1994).
[14] H. Kumomi and F. G. Shi, Phys. Rev. Lett. **82**, 2717 (1999).
[15] A. Mattoni and L. Colombo, Phys. Rev. Lett. **99**, 205501 (2007).
[16] S. Horita, H. Kaki, and K. Nishioka, J. Appl. Phys. **102**, 013501 (2007).
[17] A. A. D. T. Adikaari and S. R. P. Silva, J. Appl. Phys. **97**, 114305 (2005).
[18] G. J. Lee, S. H. Song, Y. P. Lee, H. Cheong, C. S. Yoon, Y. D. Son, and J. Jang, Appl. Phys. Lett. **89**, 151907 (2006).
[19] R. Rölver, M. Först, O. Winkler, B. Spangenberg, and H. Kurz, J. Vac. Sci. Technol. A **24**, 141 (2006).
[20] Z. Cen, J. Xu, Y. Liu, W. Li, L. Xu, Z. Ma, X. Huang, and K. Chen, Appl. Phys. Lett. **89**, 163107 (2006).
[21] L. Khriachtchev, M. Räsänen, and S. Novikov, J. Appl. Phys. **100**, 053502 (2006).
[22] V. Poborchii, T. Tada, and T. Kanayama, J. Appl. Phys. **97**, 104323 (2005).
[23] M. Zacharias, J. Bläsing, P. Veit, L. Tsybeskov, K. Hirschman, and P. M. Fauchet, Appl. Phys. Lett. **74**, 2614 (1999).
[24] T. Mchedlidze, T. Arguirov, M. Kittler, R. Roelver, B. Berghoff, M. Foerst, and B. Spangenberg, Physica E (Amsterdam) **38**, 152 (2007).
[25] T. Arguirov, T. Mchedlidze, M. Kittler, R. Rölver, B. Berghoff, M. Först, and B. Spangenberg, Appl. Phys. Lett. **89**, 053111 (2006).
[26] L. Khriachtchev, M. Räsänen, and S. Novikov, Appl. Phys. Lett. **88**, 013102 (2006).
[27] W. Cheng and S. F. Ren, Phys. Rev. B **65**, 205305 (2002).
[28] Ch. Ossadnik, S. Vepřek, and I. Gregora, Thin Solid Films **337**, 148 (1999).
[29] I. Wolf, Semicond. Sci. Technol. **11**, 139 (1996).
[30] S. Veprek, F.-A. Sarott, and Z. Iqbal, Phys. Rev. B **36**, 3344 (1987).
[31] Due to uncertainty in the exact area of the focused laser beam spot we prefer to indicate P_{LAS} instead of laser power density value in the text. Roughly, the power density for optimal SSPT at $\lambda_{LAS}=532$ nm in a $20(3Si+3SiO_2)$ MQW could be estimated as 0.2 MW cm^{-2}. Note that power density usually employed for conventional laser-induced crystallization is at least ~20 times larger, see Refs. 16–18.
[32] H. Richter and L. Ley, J. Appl. Phys. **52**, 7281 (1981).
[33] M. Lax, J. Appl. Phys. **48**, 3919 (1977).